Development of Ion Sensitive Probe and Its Application to RF Plasma Device DT-ALPHA[*]

Takahiko KOBAYASHI, Hiroyuki TAKAHASHI, Sumio KITAJIMA, Atsushi OKAMOTO[1],
Kenji TOBITA, Peerapat BOONYARITTIPONG, Takeshi SAIKYO, Yusuke ISHIKAWA,
Kenta OGASAWARA and Hidetoshi HASHIZUME

Department of Quantum Science and Energy Engineering, Tohoku University, Sendai 980-8579, Japan
[1]*Department of Applied Energy, Nagoya University, Furo-cho, Chikusa-ku, Nagoya 464-8603, Japan*

An ion sensitive probe was developed and introduced into the radio-frequency (RF) plasma source DT-ALPHA. The collector current was investigated by changing the position of the recessed collector electrode and the offset voltage to optimize these two parameters for ion temperature evaluation. It was found that the ion temperature could be overestimated when the retardation of bulk electrons is insufficient. In addition, it was also found that secondary electron emission from the collector surface results in overestimation of ion temperature. The dependence of ion temperature on RF heating power was then investigated. The ion temperature increased, and the ratio of ion temperature and electron temperature became close to 1 as RF power increased. This trend could be interpreted as a temperature relaxation between ions and electrons. The ion temperature dependence on neutral pressure was also investigated. Ion temperature monotonically decreased with increasing neutral pressure.

1. Introduction

In magnetically confined fusion research, it is very important to control the enormous heat load flowing onto the divertor plates. Detached divertor formation, which can be achieved by enhancing the volumetric recombination, is a strong candidate for the mitigation of the plasma heat load because volumetric recombination decreases the plasma pressure along magnetic field lines. To utilize volumetric recombination in the divertor region, electron energy removal is indispensable because the reaction rate of the volumetric recombination becomes large in a relatively lower electron temperature region (typically $T_e < 1$ eV), whereas the temperature of the electrons that reach the divertor region is much larger than 1 eV. Therefore, the secondary gas puffing method is widely utilized to enhance volumetric recombination [1]. To understand the mechanism of plasma detachment, investigation of the electron energy flow is required. In relatively higher electron temperature regions ($T_e > 5$ eV), electrons lose their energy through ionization and excitation. In addition, a numerical study has indicated that energy transfer from electron to ion plays an important role when electrons are cooled down below $T_e < 5$ eV [2]. Small linear devices have reported experimental results that support these energy flows [3, 4]. The amount of energy transferred from electrons to ions depends on the ion temperature T_i, as well as the electron temperature T_e. However, plasma detachment study with ion temperature measurement is insufficient, and therefore the role of ions have not been experimentally confirmed.

It is advantageous to use a small linear divertor plasma simulator for conducting experimental studies on the aforementioned subject. We have been developing a radio-frequency (RF) plasma device to study divertor plasma, and helium volumetric recombining plasma production was achieved [5]. This achievement enables us to investigate the role of ions in electron energy removal. To evaluate the amount of energy transferred among electrons, ions, and neutrals, measurement of T_i as well as T_e is required. The electron temperature where volumetric recombination is strongly enhanced can be determined by the line and continuum spectra [6]. Although ion temperature also can be determined by optical emission spectroscopy (Doppler broadening), its application to a small device is difficult because T_i in a small device is rather small. A retarding field analyzer (RFA) and ion sensitive probe (ISP) are also available for T_i measurement [7, 8]. An RFA consists of several grids and a collector, so its size is almost comparable to the diameter of the plasma produced in a small device. Therefore, the RFA would have an undesirable influence on plasma measurement when it is introduced in a small device. On the other hand, the size of an ISP is relatively smaller than that of an RFA. In addition, an ISP can measure low ion temperatures below $T_e < 1$ eV [9]. In the present work, an ISP was developed, and the first results
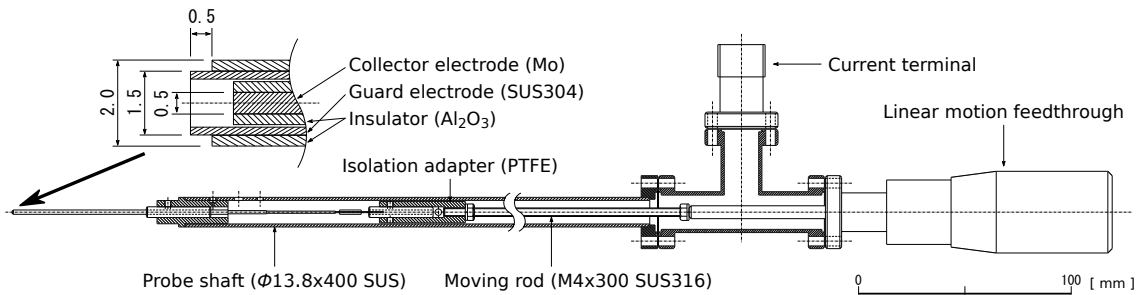
Fig. 1   Overview of the ISP developed in the present work.

of T_i measurement are reported. The design of the ISP and the experimental setup are described in Sec. 2. Then, the results of ion temperature measurement are presented and discussed in Sec. 3, followed by a summary in Sec. 4.

2. Experimental Setup

2.1   Design of the ion sensitive probe

Usually, the ion current obtained by a Langmuir probe is much smaller than that of the electrons. Therefore, it is necessary to mitigate the bulk electron inflow into an ion-collecting electrode for ion temperature evaluation. To measure bulk ions and electrons individually, an ISP that consists of an ion-collecting electrode and an electron-collecting electrode has been proposed [9]. Figure 1 shows a schematic of the ISP developed in the present work. The ISP consists of a collector electrode and a guard electrode. The collector and guard electrodes are utilized to capture ions and electrons, respectively. As illustrated in Fig. 2, the collector electrode is embedded inside the cylindrical guard electrode. Therefore, ions with larger Larmor radius can reach the collector electrode, whereas electrons with smaller Larmor radius are captured by the guard electrode. The position of the collector electrode can be adjusted by a linear motion feedthrough. In the present paper, the height of the guard electrode from the collector electrode is denoted by h. The typical magnetic field strength, electron Larmor radius, and ion Larmor radius where the ISP is installed are approximately $B = 0.15\,\text{T}$, $\rho_e = 0.5\,\text{mm}$, and $\rho_i = 3\,\text{mm}$, respectively. Therefore, a guard height approximately 1 mm is considered to be adequte. In the present experiment, the guard height was $h = 1\text{-}2\,\text{mm}$ when the ion temperature was measured. However, some electrons can still reach the collector electrode owing to the $E \times B$ drift because an equipotential surface is formed as the covering surface of an ISP [10]. In order to retard the drifted electrons, the potential of the collector electrode V_C was maintained at $V_G - V_{off}$, as shown in Fig. 3. Here, V_{off} represents the offset voltage. The collector and guard electrodes were biased individually, and the frequency of the potential sweep was 1 or 2 Hz. The values of R_C and R_G were $R_C = 1\,\text{k}\Omega$ and $R_G = 10\,\Omega$, respectively. As described in the following subsection, experiments were conducted in a radio-frequency plasma source. Therefore, normal-mode
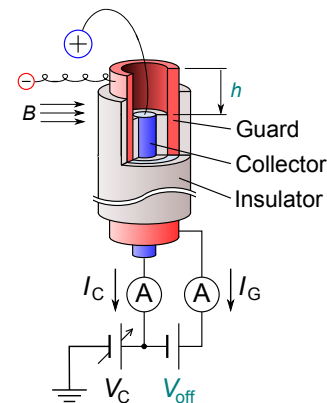
Fig. 2   Schematic of ion and electron measurements using an ISP.
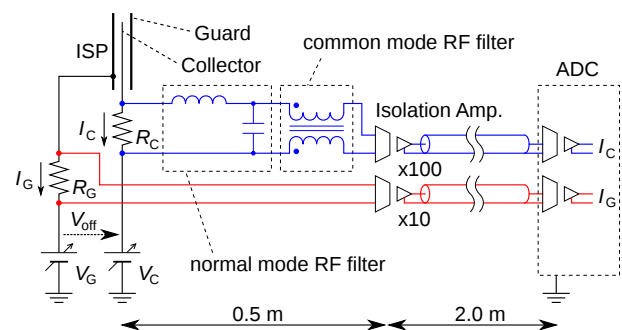
Fig. 3   The schematic diagram of the measurement circuit.

filter (LC low pass filter) and common-mode filter (choke coil) were utilized for the measurement.

2.2   RF plasma device DT-ALPHA

Experiments were performed using a DT-ALPHA device [11]. Figure 4 shows the schematic of the DT-ALPHA device. The z-axis is defined as illustrated in Fig. 4. The device consists of a quartz pipe of 36 mm inner diameter and a stainless steel (SUS) pipe of 63 mm inner diameter. The total length of the device is approximately 2 m. The plasma production method is a radio-frequency (RF) discharge. An RF power supply is connected to an antenna wound around the quartz pipe through a matching circuit. At the upstream and downstream ends of the de-
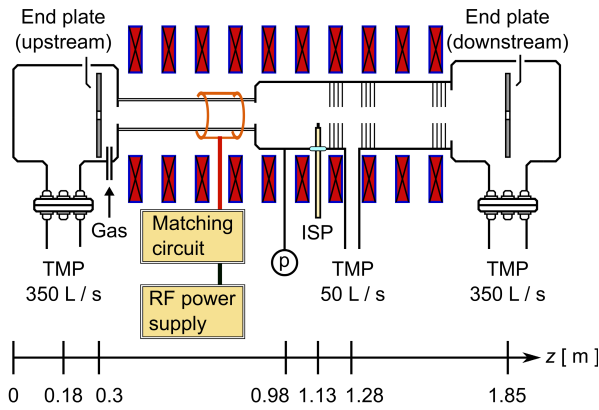
Fig. 4   Schematic of the RF plasma device DT-ALPHA.

Fig. 5   The 2D contour plot mapped with the collector current obtained with various guard heights h. Ion current was obtained in the region mapped with blue color. The region mapped with red color represents the electron current. RF heating power and neutral pressure were maintained at approximately $P_{RF} = 140$ W and $p = 1.1$ Pa, respectively.

Fig. 6   The 2D contour plot mapped with the collector current obtained with various offset voltages V_{off}. Ion current was obtained in the region mapped with blue color. The region mapped with red color represents the electron current. RF heating power and neutral pressure were maintained at approximately $P_{RF} = 140$ W and $p = 1.1$ Pa, respectively.

vice, two end-plates made of SUS are installed to terminate the plasma. Helium working gas is supplied to the device near the upstream end-plate. The ISP was installed and ion temperature measurement was conducted at $z = 1.13$ m.

3. Experimental Results and Discussion

In this section, the results of the ion temperature measurement are presented. To evaluate the ion temperature, the guard height and offset voltage should be optimized to retard the bulk electrons. Therefore, the dependence of the collector current on the guard height and offset voltage was investigated. Ion temperature measurement was then conducted by changing the RF heating power and neutral pressure.

3.1 Dependence of collector current on the guard height and offset voltage

Figure 5 shows the 2D contour map plotted using the collector current obtained for -20 V $\leqslant V_G \leqslant 80$ V, and 0 mm $\leqslant h \leqslant 2.0$ mm. The offset voltage was maintained at $V_{off} = -20$ V during the measurement. The position of the ISP was near the central region of a cylindrical plasma. The guard height h was changed with an interval of $\Delta h = 0.1$ - 0.2 mm. The electron temperature, electron density, and space potential evaluated from the I-V curve of guard current were approximately $T_e = 6$ eV, $n_e = 1 \times 10^{17}$ m^{-3}, and $V_s = -25$ V, respectively. In Fig. 5, the region where ion current was obtained is mapped with blue color. On the other hand, the region where electron current was measured is mapped with red color. To evaluate the ion temperature, the inflow of bulk electrons should be suppressed over the range of the collector potential sweep. However, as shown in Fig. 5, the electron current is clearly measured when h is smaller than 1.0 mm. On the other hand, electron current is almost zero when h is larger than 1.0 mm. Therefore, Fig. 5 indicates that in the case of $V_{off} = -20$ V, $h > 1.0$ mm is suitable for evaluating the ion temperature for these plasma parameters.
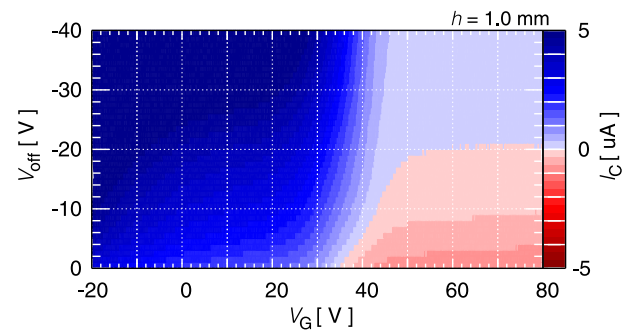
By maintaining the guard height at $h = 1.0$ mm, the dependence of the collector current on the offset voltage was also investigated. Figure 6 shows the 2D contour map plotted using the collector current obtained with -20 V $\leqslant V_G \leqslant 80$ V, and -40 V $\leqslant V_{off} \leqslant 0$ V. Here, the measurement position and plasma discharge conditions were the same as that of Fig. 5. As shown in Fig. 6, the bulk electron inflow depends on the offset voltage as well as guard height. Electron current was obtained in the region where $V_{off} \gtrsim -20$ V, whereas no electron current was observed in the region where $V_{off} < -20$ V. Therefore, Fig. 6 indicates that $V_{off} < -20$ V is suitable for ion temperature evaluation for this discharge condition and guard height.

For both $h > 1.0$ mm in Fig. 5 and $V_{off} < -20$ V in Fig. 6, ion current, which is almost independent of the col-

lector potential, was observed. Figure 7 (a) shows an I-V curve obtained with $h = 1.0$ mm and $V_{\text{off}} = -40$ V. Although the bulk electron inflow was completely suppressed, an ion current of $0.2\,\mu$A was observed above $V_C \geqslant 10$ V. This ion current I_0 became larger as the negative offset voltage increased, and its distinctive feature is that I_0 is almost independent of the collector potential. Therefore, I_0 is considered not to reflect the bulk ion inflow because it should depend on the collector potential. Based on an experiment conducted using an RFA, it has been reported that such current can be measured by the secondary electron emission [7]. Therefore, I_0 appearing in Fig. 7 (a) is also due to the secondary electrons emitted from the surface of the collector electrode. Then, the I-V curves using the non-compensated collector current (I_C) and compensated collector current ($I_C - I_0$) are compared, as shown in Fig. 7 (b). The slope of the non-compensated I-V curve (red circles) yielded an ion temperature of $T_i = 4.0$ eV, whereas that of the compensated one (blue circles) yielded $T_i = 2.3$ eV. This result indicates that the ion temperature can be overestimated by the secondary electron emission. The influence of the guard height, offset voltage, and compensation of the I-V curve on ion temperature evaluation are summarized in the following subsection.

The space potential corresponding to Fig. 7 is approximately $V_s = -25$ V. Therefore, T_i is expected to be obtained using the slope near $V_C = -25$ V. However, as shown in Fig. 7 (b), T_i was evaluated using the slope where the collector potential is larger than the space potential, instead of using the slope near V_s because the I-V curve seems to deviate from the Maxwellian distribution near V_s. One possible reason of this deviation is the space-charge limit. According to Brunner *et al.* [12], the shape of an I-V curve is affected when a probe is limited by the space-charge. In Ref. 12, a critical bias voltage $V_{\text{crit}} = d/4\sqrt{n_i k_B T_i / \varepsilon_0}$ is proposed to avoid the influence of space-charge and to obtain reliable ion temperature. Here, d represents the distance between a guard electrode and a recessed collector electrode. ε_0 is the permittivity of free space. Utilizing $n_i = 1 \times 10^{17}$ m^{-3}, $T_i = 2.3$ eV, and $d = 1$ mm, we obtain $V_{\text{crit}} \sim 16$ V. Unfortunately, it was difficult to evaluate T_i from the slope above $V_C > 16$ V; hence, T_i was obtained using the slope around $V_C = 5$ V. Similarly, T_i presented in the following subsections were also obtained from the slope where the collector potential was larger than the space potential. Another work on ISP measurement indicated that large offset voltage leads to an anomalous I-V curve, which seems to involve high energy tail components [13]. However, a clear tail component was not observed in the present study.
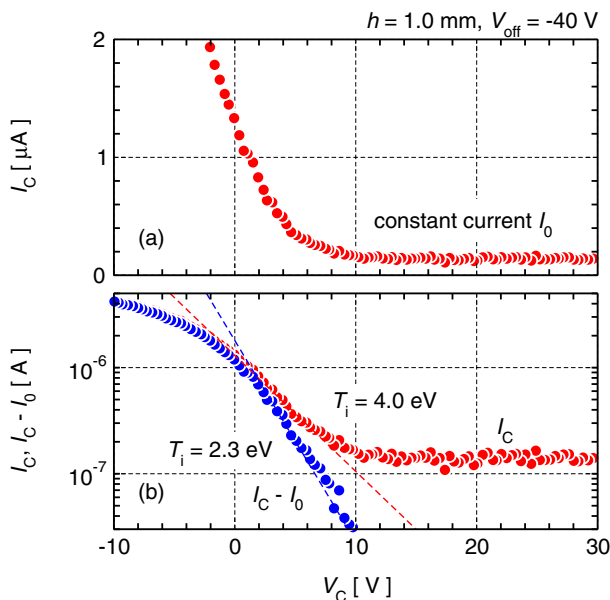
3.2 Influence of the guard height and offset voltage on ion temperature evaluation

The influence of secondary electron emission and bulk electron inflow on ion temperature evaluation was investigated for $h = 1.0$ mm and 2.0 mm. The results are summarized in Fig. 8. The horizontal axis in each figure represents the offset voltage. As described in Sec. 3.1, the electron current is observed when V_{off} is insufficient. The electron

Fig. 7 I-V curves of (a) linear plot and (b) semi-log plot. The red and blue dots represent the I-V curves obtained using non-compensated collector current (I_C) and compensated collector current ($I_C - I_0$), respectively. RF heating power and neutral pressure were maintained at approximately $P_{\text{RF}} = 140$ W and $p = 1.1$ Pa, respectively.
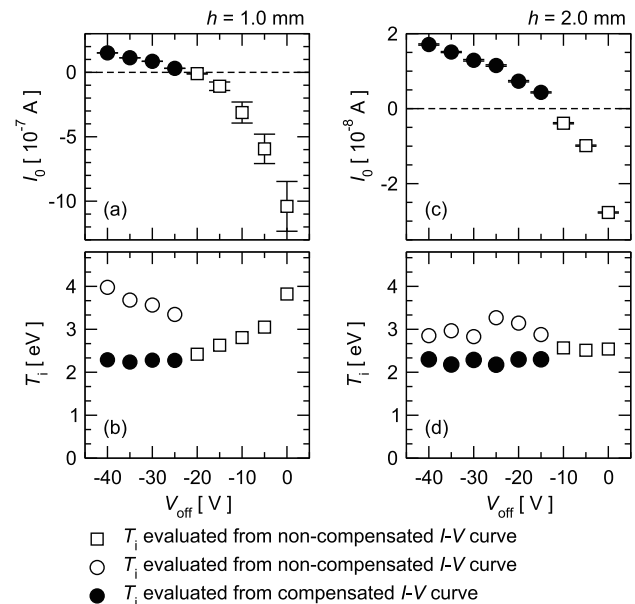
Fig. 8 Collector current I_0 and ion temperature T_i as a function of the offset voltage. Left-hand side column and right-hand side column correspond to $h = 1.0$ mm and $h = 2.0$ mm, respectively. RF heating power and neutral pressure were maintained at approximately $P_{\text{RF}} = 140$ W and $p = 1.1$ Pa, respectively.

current became saturated as the collector potential became large. The open squares in Fig. 8 (a) correspond to this electron saturation current. On the other hand, the filled circles in Fig. 8 (a) represents the collector current due to the secondary electron emission. The open squares and circles in Fig. 8 (b) represent the ion temperature T_i evaluated from the I-V curves obtained for these conditions. Although the inflow of bulk electrons makes T_i evaluation inadequate, the ion temperature was approximately obtained. In this case, I_0 has a negative value, so $-I_0$ was added to the I-V curve and T_i was obtained using its slope. In principle, T_i is independent of the measurement parameters, namely V_{off} and h. However, as shown in Fig. 8 (b), T_i obtained from these I-V curves clearly depends on the offset voltage. As described above, the positive collector current is due to the secondary electron emission. Then, the current was subtracted from the I-V curve, and the ion temperature was evaluated. The filled circles in Fig. 8 (b) represent the ion temperature obtained from the compensated I-V curve. T_i evaluated from the compensated I-V curve showed an almost constant value of $T_i = 2.3$ eV. A similar investigation was conducted using $h = 2.0$ mm. Figure 8 (c) and Fig. 8 (d) summarize the results. As shown in Fig. 8 (c), the collector current I_0, which is due to the bulk electron inflow and secondary electron emission, is much smaller than that in Fig. 8 (a). Although the influence of the secondary electron emission on T_i evaluation is relatively smaller than that for $h = 1.0$ mm, T_i obtained using non-compensated I-V curves varies slightly, as shown in Fig. 8 (d). However, T_i obtained from compensated I-V curves is independent of the offset voltage and has almost comparable value to that in Fig. 8 (b).

3.3 Ion temperature dependence on RF power

Figure 9 shows the electron density n_e, electron temperature T_e, ion temperature T_i, and temperature ratio T_i/T_e as a function of RF power P_{RF}. T_e and n_e were evaluated using the I-V curves obtained by the guard electrode. The helium neutral pressure was 0.56 Pa. As the RF power increased, the electron density monotonically increased from $n_e = 3 \times 10^{15}$ m^{-3} to $n_e = 8 \times 10^{16}$ m^{-3}. At relatively lower RF power, the electron temperature was approximately $T_e = 10$ eV and decreased to $T_e = 6$ eV with increasing RF power. As shown in Fig. 9 (b), T_i at lower P_{RF} is approximately 3 eV. As P_{RF} increased, T_i increased gradually and became approximately 5 eV near $P_{RF} = 100$ W. The dependence of the temperature ratio T_i/T_e is shown in Fig. 9 (c). Although T_i/T_e at $P_{RF} = 1$ W was approximately 0.4, it increased toward the high RF power region. Finally, T_i/T_e exceeded 0.7. In a DT-ALPHA device, ions obtain their energy mainly through the electron-ion collision because no ion heating system is equipped. One of the possible reasons for the increase in the ion temperature is the electron-ion temperature relaxation. Then, T_i/T_e was again plotted as a function of
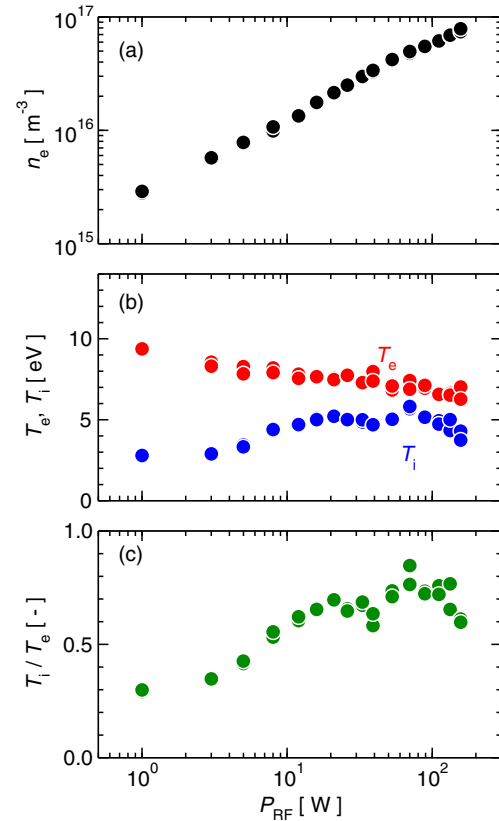
Fig. 9 Dependence of (a) the electron density n_e, (b) the electron temperature T_e and the ion temperature T_i, and (c) the temperature ratio T_i/T_e on the RF power P_{RF}. Neutral pressure was maintained at approximately 0.56 Pa.
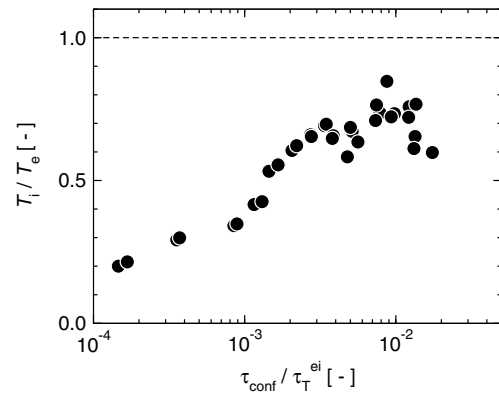
Fig. 10 Dependence of T_i/T_e on τ_{conf}/τ_T^{ei}.

τ_{conf}/τ_T^{ei}, as shown in Fig. 10. Here, τ_{conf} and τ_T^{ei} represent the plasma confinement time and the electron-ion temperature relaxation time, respectively. In a DT-ALPHA device, the typical ion Mach number α is $\alpha = 0.1$ [14]. Using ion sound velocity $C_s = \sqrt{e(T_e + T_i)/m_i}$, τ_{conf} is given as

$$\tau_{conf} = \frac{l}{\alpha C_s}. \tag{1}$$

Here, l represents the distance between the plasma production region and measurement position. In the present study,

the value of l was chosen as 0.5 m. Note that the ion temperature and electron temperature obtained from the ISP were used for evaluating C_s. Electron-ion temperature relaxation time τ_T^{ei} is given as

$$\tau_T^{ei} = \frac{3\sqrt{2\pi}\pi\varepsilon_0^2\,m_i m_e}{n_i Z_i^2 e^4 \ln\Lambda}\left(\frac{T_e}{m_e}+\frac{T_i}{m_i}\right)^{3/2}. \qquad (2)$$

Here, Z_i, e, and $\ln\Lambda$ represent the ion charge number, electron charge, and Coulomb logarithm, respectively. Ion density was assumed to be equal to electron density n_e. In addition to the ion sound velocity, T_e, T_i, and n_e obtained using the ISP were utilized for τ_T^{ei} evaluation. As shown in Fig. 10, T_i/T_e increased gradually as τ_{conf}/τ_T^{ei} increased. At $\tau_{conf}/\tau_T^{ei} = 10^{-2}$, T_i/T_e becomes approximately 0.8. This result indicates that the increase in ion temperature was due to the temperature relaxation between electrons and ions. Although temperature relaxation seems to be a possible interpretation of the results, a more detailed understanding is required because τ_{conf} is much smaller than τ_T^{ei} even though $T_i/T_e \sim 0.8$. As described above, T_e, T_i, and n_e utilized for each calculation were obtained by the ISP ($z = 1.13$ m). However, temperature relaxation proceeds while ions and electrons move from the plasma production region to the measurement position. Therefore, a more detailed understanding is expected to be obtained by considering the axial distribution of the electron temperature and ion temperature.

3.4 Ion temperature dependence on neutral pressure

The ion temperature was also measured by changing the neutral pressure from 0.37 Pa to 2.8 Pa. Figure 11 shows the electron density n_e, electron temperature T_e, ion temperature T_i, and temperature ratio T_i/T_e as a function of neutral pressure. Here, the neutral pressure was measured at $z = 0.98$ m. The RF power was maintained at $P_{RF} = 140$ W during measurements. As the neutral pressure increased, the electron density increased from $n_e = 0.4 \times 10^{17}$ m^{-3} to more than $n_e = 1 \times 10^{17}$ m^{-3}. The electron temperature monotonically decreased with increasing pressure. The increase in n_e and decrease in T_e observed in $p < 1$ Pa can be interpreted by the electron impact ionization. However, n_e had no clear dependence on neutral pressure in the region where $p > 1$ Pa. The cross section of the electron impact ionization σ_{ion} is strongly dependent on the electron energy. At around $T_e = 10$ eV, the rate coefficient $\langle\sigma_{ion}v\rangle$ decreases considerably when the electron temperature decreases. Therefore, the decrease in electron temperature is considered to be a possible reason for the trend observed in $p > 1$ Pa. In addition to the electron temperature, the ion temperature also decreased monotonically. The T_i/T_e ratio decreased slightly as the neutral pressure increased. Electrons exhaust their energy due to ionization, excitation, and temperature relaxation between ions. Although ions can obtain energy through temperature relaxation, their energy also moves to neutral particles
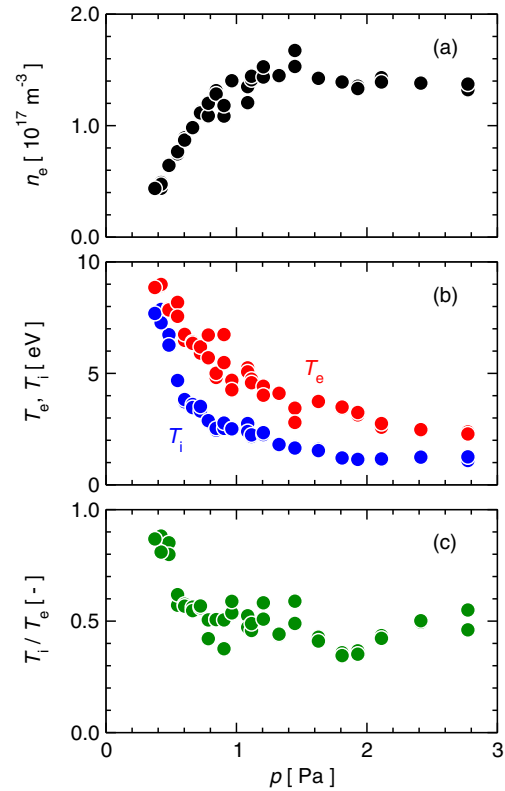
Fig. 11 Dependence of (a) the electron density n_e, (b) the electron temperature T_e and the ion temperature T_i, and (c) the temperature ratio T_i/T_e on the neutral pressure p. RF power was maintained at approximately 140 W.

through the charge-exchange interaction. The decrease in ion temperature reflects ion cooling due to the charge-exchange interaction. Quantitative evaluation of the energy balance among electrons, ions, and neutrals will be our future work.

4. Summary

An ISP was developed and introduced to the radio-frequency plasma source DT-ALPHA. To optimize ion capturing, the guard height of the ISP was designed to be adjustable. The first ion temperature measurement in the DT-ALPHA device was then conducted using the ISP. To determine the optimal guard height and offset voltage for ion temperature evaluation, the collector current was measured by changing these parameters. The collector current was clearly dependent on the guard height and offset voltage, and it was found that the typical guard height and offset voltage required for retarding the bulk electron inflow are 1.0 mm and −20 V, respectively. The influence of bulk electrons and secondary electrons on ion temperature evaluation was also investigated. It was found that the ion temperature is overestimated when retardation of the bulk electrons is insufficient. In addition, it was also found that ion temperature can be overestimated because of the secondary electron emission even though the inflow of bulk electrons is suppressed. Then, the dependence of ion temperature

on RF power was investigated. Although the ion temperature was smaller than the electron temperature at relatively lower RF power, it increased as RF power increased. One possible interpretation of this trend is the temperature relaxation between electrons and ions. However, a more detailed investigation is required to understand the results, because the electron-ion temperature relaxation time was still much longer than the plasma confinement time even though in a relatively higher RF power region. The ion temperature dependence on neutral pressure was also investigated. Ion temperature monotonically decreased with increasing neutral pressure. The charge-exchange interaction between bulk ions and neutral atoms could account for this trend. To understand the behavior of ion temperature against RF power and neutral pressure, an understanding of the energy transfer among electrons, ions, and neutrals is necessary. This will be investigated in our future work. In addition, we will also conduct ion temperature measurement in volumetric recombining plasma.

Acknowledgment

[1] N. Ohno, Plasma Phys. Control. Fusion **59**, 034007 (2017).
[2] N. Ohno, S. Mori, N. Ezumi, M. Takagi and S. Takamura, Contrib. Plasma Phys. **36**, 339 (1996).
[3] N. Ezumi, S. Mori, N. Ohno, M. Takagi, S. Takamura, H. Suzuki and J. Park, J. Nucl. Mater. **241-243**, 349 (1997).
[4] H. Takahashi, A. Okamoto, T. Miura, D. Nakamura, P. Boonyarittipong, S. Sekita and S. Kitajima, Plasma Fusion Res. **11**, 2402059 (2016).
[5] H. Takahashi, A. Okamoto, Y. Kawamura, T. Kumagai, A. Daibo and S. Kitajima, Fusion Sci. Technol. **63**, 404 (2013).
[6] D. Nishijima, U. Wenzel, K. Ohsumi, N. Ohno, Y. Uesugi and S. Takamura, Plasma Phys. Control. Fusion **44**, 597 (2002).
[7] C. Böhm and J. Perrin, Rev. Sci. Instrum. **64**, 31 (1993).
[8] I. Katsumata and M. Okazaki, Jpn. J. Appl. Phys. **6**, 123 (1967).
[9] I. Katsumata, Contrib. Plasma Phys. **36** S, 73 (1996).
[10] N. Ezumi, Contrib. Plasma Phys. **41**, 488 (2001).
[11] A. Okamoto, K. Iwazaki, T. Isono, T. Kobuchi, S. Kitajima and M. Sasao, Plasma Fusion Res. **3**, 059 (2008).
[12] D. Brunner, B. LaBombard, R. Ochoukov, R. Sullivan and D. Whyte, Plasma Phys. Control. Fusion **55**, 125004 (2013).
[13] N. Ezumi, Zh. Kiss'ovski, W. Bohmeyer and G. Fussmann, J. Nucl. Mater. **337-339**, 1106 (2005).
[14] T. Kumagai, A. Okamoto, H. Takahashi, A. Daibo, T. Takahashi, S. Tsubota and S. Kitajima, JPS Conf. Proc. **1**, 015043 (2014).